

The Philips logo is displayed in a white rounded rectangle on a blue background. The background of the entire top section is a photograph of a man in a dark shirt talking to a woman in a light blue lab coat in front of an MRI machine's gantry.

PHILIPS

Ingenia MR-RT

MR Systems

MR-only simulation for radiotherapy planning

White paper: Philips MRCAT for prostate dose calculations using only MRI data

M. Köhler, T. Vaara, M. Van Grootel, R. Hoogeveen, R. Kemppainen, S. Renisch

Highly targeted treatment planning is at the foundation of successful radiotherapy. With its superb and tunable soft-tissue contrast, MRI has in recent years emerged as an imaging modality to drive delineation accuracy of targets and organs at risk. With the introduction of the first commercially available MR-only simulation package, Philips continues to pave the way for the adoption and implementation of MRI in radiation treatment planning. Philips MR-only simulation offers a single-modality approach that provides both excellent soft-tissue contrast for target delineation and density information for treatment planning for prostate cancer.

MR simulation for radiotherapy treatment planning

Imaging forms a cornerstone of modern radiation therapy (RT) by providing essential information on 3D tumor position and identification of organs at risk (OAR). Where Computed Tomography (CT) has since long been the primary imaging modality, the recent emergence of Magnetic Resonance (MR) imaging within the RT environment is driven by the need for more accurate target definition. Besides its superior soft-tissue contrast as compared to CT, other acknowledged benefits of MRI include functional imaging for target delineation and dynamic imaging techniques for motion assessment, all without adding radiation dose (see Figure 2). The availability of an MRI system in the RT department will increase the ability to leverage these benefits not only for target delineation, but also for treatment response assessment and adaptive therapies [1].

Although diagnostic images are routinely considered for treatment planning, a dedicated MR simulation approach is necessary to meet the specific requirements of RT [2]. Imaging the patient in the RT treatment position is important for co-registration and total accuracy [3]. Vendors have introduced RT-dedicated MR simulation systems with 70 cm bore size and MRI compatible immobilization equipment, including flat table overlays and coil support solutions. The latest Philips Ingenia MR-RT solution provides an integrated, flat RT couchtop – not an overlay – which completely replaces the diagnostic couchtop for patient positioning close to the Posterior coil for improved SNR and more bore space for patient positioning (see Figure 1).



Figure 1: the Ingenia MR-RT as a dedicated platform for Radiation Oncology with MR-RT CouchTop, Coil Support and optional external laser positioning system (ELPS)

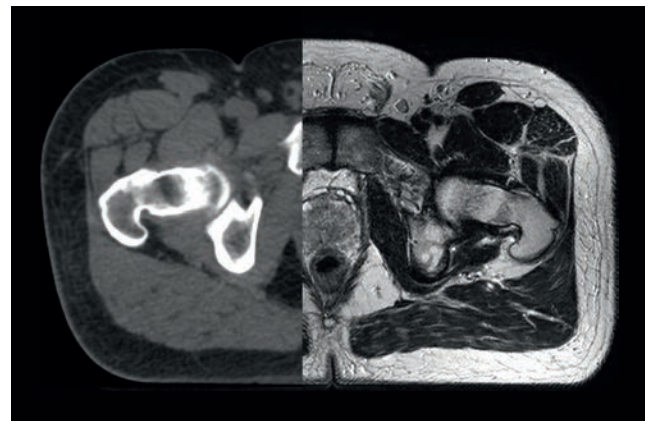
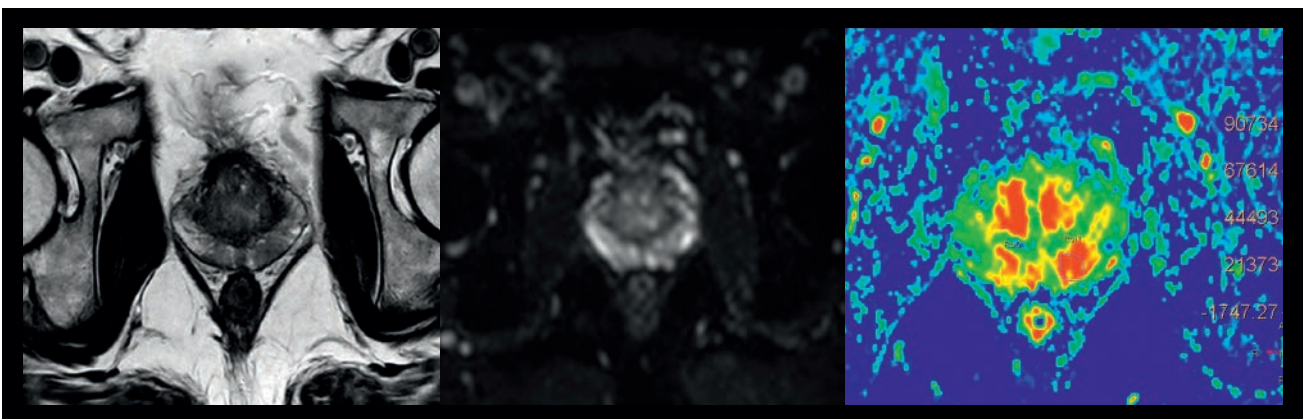


Figure 2: MRI offers excellent soft-tissue contrast and a wide range of image contrasts for tumor visualization. Upper image: CT and MR image of a prostate patient acquired in the treatment position. Courtesy of Beaumont Health System, Michigan, USA. Ingenia MR-RT 3.0T. Lower image: different MR image contrasts (T2W, DWI and DCE) of the prostate. Courtesy of Clinique Jules Verne, Nantes, France. Ingenia 1.5T.



Several years ago, adoption of MRI was hampered by the existence of geometric distortions caused by nonlinearity of the gradients and magnet field inhomogeneity. Although still a point of attention, the MR-RT systems today have greatly improved gradient linearity and routinely apply gradient distortion correction, thus minimizing any effect of potential system-specific distortions.

As MRI does not intrinsically provide electron density information as input for dose calculations, most clinical treatment planning workflows include registration of an MRI dataset to a primary CT dataset. MRI-based information on tissue characterization and tumor delineation is registered to a primary CT dataset, which provides the electron density information for dose calculations. This approach nicely combines the complementary benefits of both CT and MRI, yet puts pressure on workflows, patients, and costs. Next to being labor-intensive, CT-MRI image registration also

introduces uncertainties [3]. Errors in the alignment of MRI and CT images series in the treatment preparation stage propagate as a systematic error, usually accounted for by increased margins. The latter follows the patient throughout the entire treatment period. An MRI-only simulation workflow can virtually eliminate all technical and economic issues related to an MR-CT multi-modality imaging workflow for specific anatomical sites (see Figure 3). Such a workflow requires MRI to provide not only information on tumor volume and location, but also the electron density information required for dosimetry (see Figure 4). In addition, the generated density maps should also provide the means to replace the CT from the positioning process during treatment setup.

This article describes the Philips MRCAT (Magnetic Resonance for Calculating Attenuation) solution for an MR-only based dose planning approach for external beam radiation therapy (EBRT).

CT-MR registration workflow



MR-only simulation workflow



Figure 3: schematic representation of the main steps in the conventional CT-MR based workflow and the MR-only simulation workflow. MR-only simulation excludes CT imaging and CT-MR registration.

MR-only simulation for prostate

Perform prostate dose calculations based on MR data only

Figure 4: Schematic representation of the MR-only sim workflow with a dose plan based on T2W imaging data and MRCAT-based density information

MR-only simulation for prostate radiotherapy treatment

Prostate cancer has one of the highest incidence rates of all cancer types in Europe [4], and for a large number of prostate cancer patients, radiation therapy is included in the treatment strategy. The prostate has been the subject of growing interest in using MRI to improve anatomical accuracy of the prostate and surrounding organs, with the aim to improve accuracy of planning delineations. Furthermore, intraprostatic lesions can be identified on MRI, suggesting that focal therapy or boosting could benefit from using MR images for planning [5]. These were the motivating factors behind the choice for prostate as the first application for the commercial MR-only simulation product release.



MR-only simulation into clinical practice

Recent advances in technological development in dose delivery hardware and software, including IMRT and VMAT, enable delivery of external RT treatments with high precision. The overall accuracy requirement for the delivered dose is usually set to 5%, which requires a typical accuracy of the computed dose distributions of between 1-2% [6]. To achieve this, patient-specific inhomogeneity correction is applied in dose computations. Absorption of radiation in human tissue is a complex process where highly energetic primary photons transfer their energy to electrons contained in matter via collisions. The absorption rate is dependent on the medium's electron density. CT provides this electron density information since its contrast is based on attenuation of ionizing radiation. MR images do not intrinsically contain electron density information. When MRI is used for RT planning without an accompanying CT scan, electron density information must be obtained via other means. Our solution for the density assignment, MRCAT, is built around a model-based classification method and it is based on mDixon imaging.

Besides generating electron density information, there are more requirements for enabling MRI as a standalone imaging modality for RT planning. RT is a multi-disciplinary, multi-phase process where the chain from dose prescription to the delivery of treatment must be refined to reduce sources of error. Any addition of a new method such as MR-only simulation where MRI is used as the primary, and only, imaging modality for RT planning, must be carefully analyzed in terms of impact on overall accuracy and efficiency. Workflow aspects, such as patient immobilization, patient marking, position verification, and the option to generate digitally reconstructed radiographs (DDRs), need to be considered, as well as acceptance of the density information generated by MR images in treatment planning systems (TPS).

This white paper explains each step in our solution toward successfully using MR-only treatment planning.

MR imaging strategies for MR-only simulation

MR-only simulation demands a dedicated imaging approach. Time for imaging must be as short as possible to help keep workflows efficient, patients comfortable, and organ movement to a minimum. The minimum set of scan protocols needed for the Philips MR-only approach are a source for MRCAT generation, a scan for visualization of internal markers, and the scan protocol for target and OAR contouring (see Table 1).

Scan protocols specific to treatment planning must also be optimized. Speed and robustness are essential. Other requirements include high spatial resolution in three dimensions (preferably with isotropic voxels), a large FOV, and contrast tailored to the tumor and OAR. Consistency is another important consideration. The consistent use of scan protocols helps maintain control over the accuracy of skin and other air-tissue interfaces. Since the most sensitive protocols, such as MRCAT, allow for fewer modifications, they are designed to deliver reproducible results independent of user experience.

Fast, robust imaging protocols

Dedicated imaging protocols are needed to obtain an accurate CT equivalent radiation attenuation map with MRI. The different tissues types must be automatically distinguished and assigned with appropriate Hounsfield units. Most approaches previously described in the scientific literature require either manual segmentation or multiple scans that must be registered in order to derive this information [7]. With the Philips MRCAT solution, a single mDIXON MRI sequence is used to generate electron density information, thereby removing the risk of inter-sequence registration uncertainty. In the mDIXON approach, two echoes are acquired, allowing water, fat, and in-phase images to be derived from the same acquisition by using the frequency shift of the fat and water protons.

The mDIXON scan used by the MRCAT algorithm is designed to have high geometric accuracy by the choice of short echo times and high bandwidth. The spatial resolution is chosen to be sufficiently high to allow reliable segmentation of the bones needed for accurate dose planning.

Implantable markers are often used in external beam RT for target positioning to enable inter-fraction organ motion control. The markers are often visible in the mDIXON water and in-phase images acquired for MRCAT. However, a verification scan may be needed to confirm the exact location of the markers. To this end, imaging protocols sensitive to the local magnetic field disturbances can be used in which the markers appear as signal voids inside the prostate [8]. Our choice for marker detection is a bFFE/FFE 3D scan protocol which provides high SNR and completes in less than two minutes. Fast scan time helps avoid inter-scan organ motion.

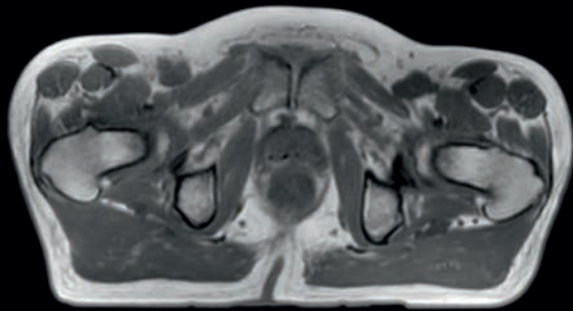
T2-weighted TSE images allow manual delineation of the prostate including the prostatic apex and seminal vesicles. The OARs (bladder, rectum, and femur heads) can be delineated with the T2 image, and the T1-weighted in-phase image contrast derived from the mDIXON may provide valuable additional anatomical information. An overview of the acquired images is given in Figure 5 and Figure 6.

MR-only scanning protocol includes

- **dedicated 3D MRCAT source sequence** as input for generation of density information for dose calculations
- **anatomical information for delineation** of target and critical structures
- **prostate marker visualization** for position verification

Purpose	Protocol	Weighting	FOV (AP*LR*FH)	Resolution (recon, mm)	TE (ms)	TR (ms)	Protocol time
Survey	Survey+ scan prep						
MRCAT source	mDIXON FFE3D	T1	350*450*300	1.04*1.04*2.50	1.2/3.9	2.5	2:17
Marker visualization	b-FFE3D	T2/T1	180*180*90	0.56*0.56*1.00	3.6	7.2	1:46
Target contouring	TSE3D	T2	350*450*300	0.56*0.56*1.20	258	2000	7:02
Total scanning duration							~ 12 min

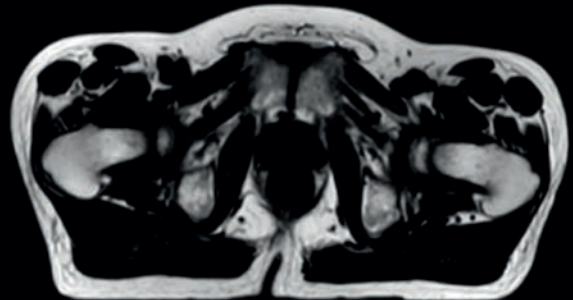
Table 1: The details of the MR-only simulation scan protocols for prostate application (Ingenia 3.0T)



in-phase



water



fat



T2W

Figure 5: The mDIXON FFE3D MRCAT source images give in-phase, water, and fat images, while the TSE3D gives the T2 contrast.

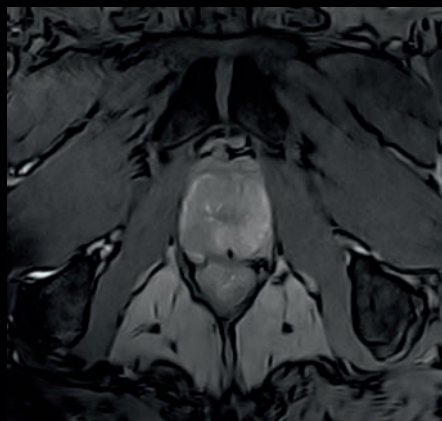


Figure 6: Left: The b-FFE3D gives the high resolution needed for detecting possible gold seeds. Right: This CT image shows the prostate marker.

Accurate MR imaging for MR-only simulation

Historically, geometric accuracy has been a limitation for the applicability of MRI in RT. In recent years, major improvements in geometric fidelity have been obtained, and contemporary Ingenia scanners are able to produce the accuracy needed for most RT applications.

Geometric distortions can originate from two main sources: system and patient (see Figure 7). Distortions caused by gradient field nonlinearity and static magnetic field (B0) inhomogeneity can be characterized, measured, and, finally, corrected accurately, such as with 3D gradient distortion correction. However, less predictable distortions can be caused, such as by tissue susceptibility differences and MRI-incompatible accessories accidentally used in the MRI. The patient-related distortions can be measured, but they depend on the individual patient and imaging setup. Fortunately, MR imaging protocols can be optimized to minimize the effect of susceptibility-related distortions by wisely choosing water-fat shift parameters, for example. The MR-only simulation scanning protocol has been designed with the strict accuracy requirements of RT in mind.

Since geometric inaccuracies can introduce systematic errors, periodic and frequent quality assurance (QA) of geometric fidelity is needed. For the assessment of geometric accuracy, Philips provides a dedicated QA phantom and software in addition to the standard image quality QA tools that come with the Ingenia MR-RT (see Figure 8).

Measurements were performed in-house with a specially developed 3D phantom in the Ingenia 1.5T and Ingenia 3T systems using MRCAT source sequences. Calibration of the geometric accuracy of the phantom itself is crucial for reliable measurement and susceptibility effects due to phantom materials shall also be minimized. The total geometric accuracy (which includes B0 non-uniformity and residual gradient distortion errors as well as residual phantom susceptibility errors) was measured to be in this case:

1.5T:

- MRCAT provides < 0.54 +/- 0.12 mm total geometric accuracy of image data in < 20 cm Diameter Spherical Volume (DSV)
- MRCAT provides < 0.9 mm +/- 0.32 mm total geometric accuracy of image data in < 40 cm Diameter Spherical Volume (DSV)*

3.0T

- MRCAT provides < 0.8 +/- 0.12 mm total geometric accuracy of image data in <20 cm Diameter Spherical Volume (DSV)
- MRCAT provides < 1.4 +/- 0.32 mm mm total geometric accuracy of image data in < 40 cm Diameter Spherical Volume (DSV)*

* Limited to 32 cm in z-direction in more than 95% of the points within the volume

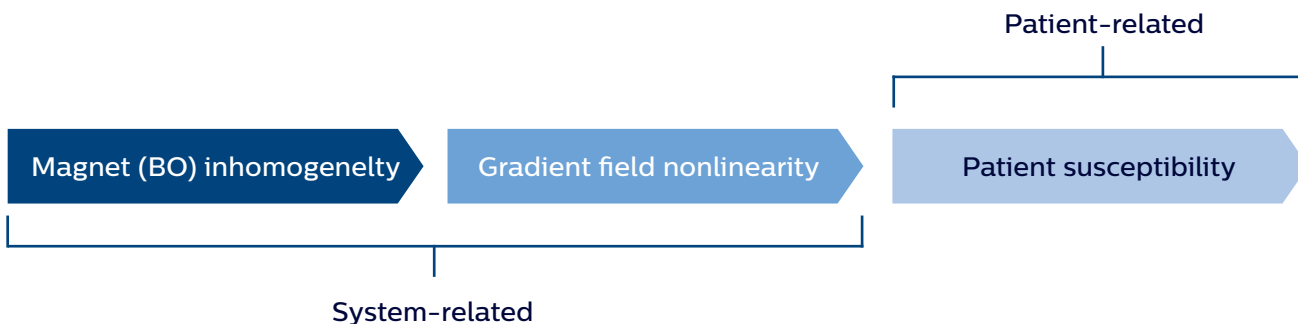


Figure 7: Sources of geometric distortion in MR



Figure 8: The geometric distortion phantom travels through the magnet’s bore and a scan protocol maps it in 3D in seven parallel volumes. Automated analysis provides accuracy contours. In addition, the phantom can be used to assess the distortion in sagittal and coronal planes.

Generation of density maps

Philips MRCAT approach

The general problem in the generation of density maps based on MR images is that due to imaging physics, tissues with very different densities (air and cortical bone tissue, for instance) may give similar MR signal intensities. To resolve this ambiguity, the Philips MRCAT approach for electron density assignment to MR images uses an accurate and robust segmentation of bone structures and soft tissue. Within the individual compartments (bone and soft tissue), the correlation between the MR signal intensities and the electron density is much better. As a result, voxels can be assigned density values based on their intensity with an accuracy sufficient for treatment simulation.

Thus, in the MRCAT application, CT-like density maps are generated from mDIXON images in a two-step approach. In the first step, the contents of the MR image are categorized into five classes (air, fat, water-rich tissue, spongy bone, and compact bone).

In the next step, each voxel is assigned a density value (pseudo-HU value) based on a combination of average population values and literature values [9] [10] [11], (see Figure 10).

Tissue classification

The membership of a certain voxel to a class is determined by the following procedure: First, the body outline (skin surface) of the patient is determined. The voxels outside

of this body outline are classified as air. Second, all bone structures are segmented inside the body using the multiple contrasts provided by the mDIXON scan. Both the bone and outline segmentation employ a model-based segmentation approach trained on patient and volunteer mDIXON image datasets. The model is adapted to an actual patient image using features (such as gray value edges) found within the image, while at the same time, a constraint for the shape of the segmented structure prevents the segmentation from being attracted to the wrong position [12] [5].

The voxels inside the body outline, but outside of the bone segmentation, are considered soft tissue. This is further subdivided according to the intensities in the water and fat 3D images; voxels with a higher fat than water content are classified as fat, whereas voxels with higher water content are classified as water-rich tissue.

Voxels inside the bone segmentation are assumed to contain either compact or spongy bone; the distinction is made based on the voxel intensity of the in-phase image. On a mixture of patient and volunteer images, the bone segmentation showed an accuracy of less than 1 mm RMS error when compared to manual bone delineations. This is a remarkably good result given the reconstructed voxel size of $1.5 \times 1.5 \times 2.5 \text{ mm}^3$ for the analyzed datasets.

The algorithm pipeline is summarized in Figure 9.

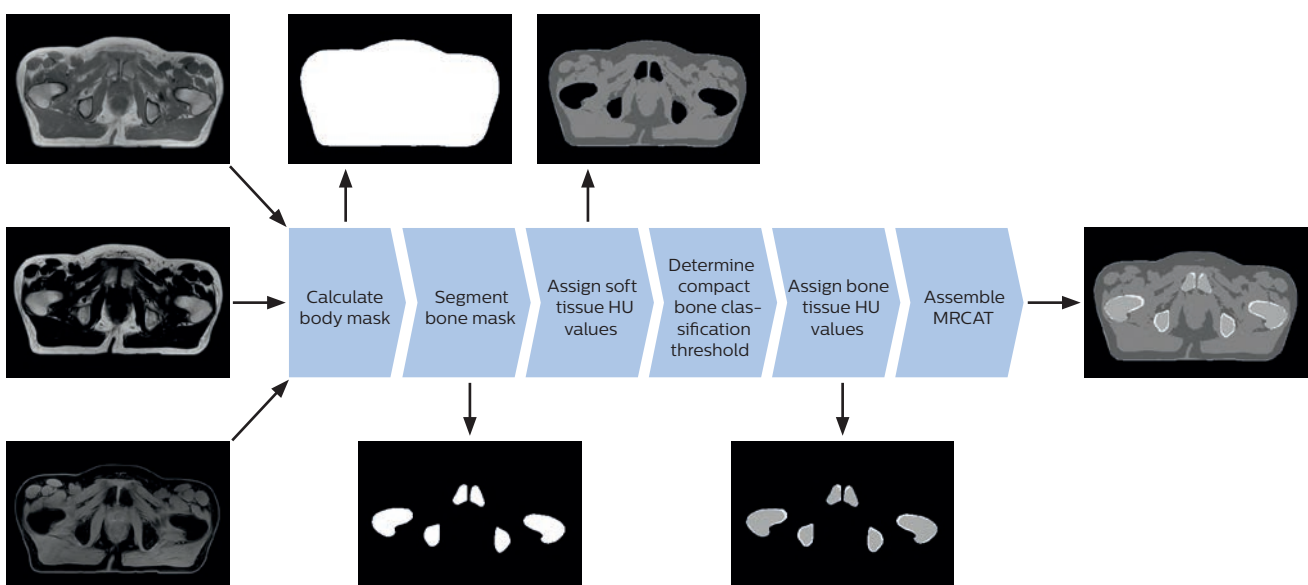


Figure 9: Algorithm pipeline showing the calculation flow from mDIXON images with the calculated MRCAT images as the end result

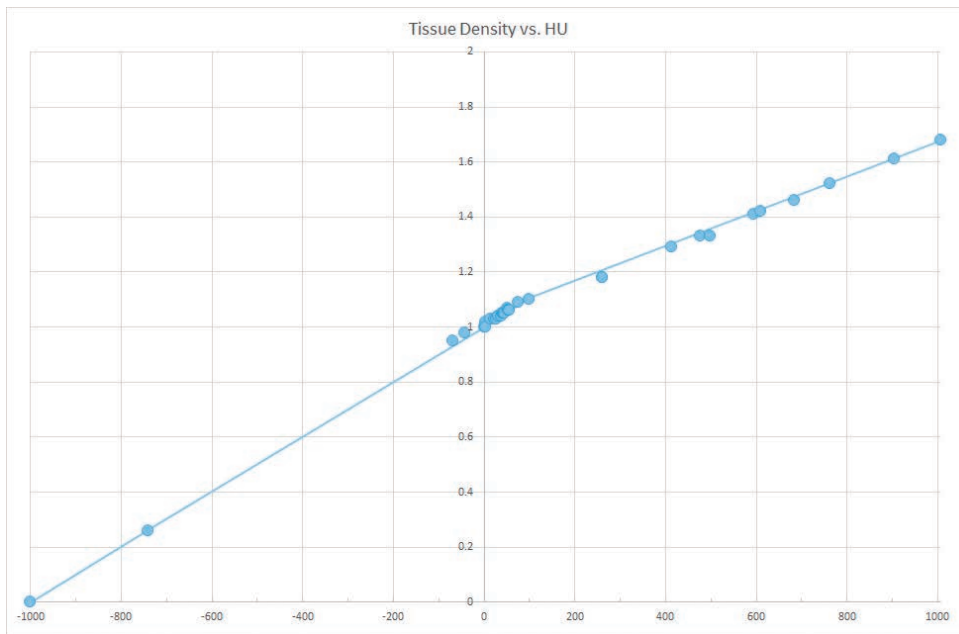


Figure 10: Visual representation of HU versus density values for human tissues. Data adapted from literature [9], [10], [11]

MRCAT post-processing starts automatically after the collection of mDIXON images is complete. Other scan protocols, such as the T2 acquisition, can run during the post-processing, which takes place in the background parallel to image acquisition and therefore does not add time to the overall session.

This approach also implements a method for automatic failure detection which may be useful in detecting errors, such as selection of a too-small FOV or intra-scan movements which cause segmentation to fail. This adds to, but does not replace, a recommended visual inspection by the end user for the quality and completeness of the MRCAT images.

Alternative MR-only strategies

Multiple methods for automated generation of CT-equivalent information derived from MRI have been suggested in the literature. The most straightforward approach is to assign one density value for the whole (MRI-contoured) anatomy, but this approach has the obvious limitations of lacking bone outlines that can be used for position verification. In addition, the lack of information on tissue heterogeneity causes compromised dose calculation accuracy.

One approach to resolve the aforementioned ambiguity between MR signal intensity and electron density is to use an atlas-based method (such as the one described by J. A. Dowling [13]). In this approach, a population-average density map (the atlas) is constructed by registering a cohort of CT images non-rigidly onto each other and combining those. This average density map is then mapped to a particular patient by a non-rigid registration. Various publications exist that use machine-learning techniques to augment the atlas registration (such as the approach described by M. Hofmann [14]). However, the main drawback of these methods is the uncertainty in image registration; achieving subvoxel accuracy in a robust fashion is rather challenging.

Another approach for the resolution of the MR/density ambiguity is to extract some signal from bone structures and combine this with another MR contrast. Cortical bone does not yield signal in traditional MRI scans due to its very short T2*-time. However, by sampling MR signal just after the excitation pulse, it is possible to detect MR signal even from dense bone. This can be achieved by ultra-short echo time (UTE) imaging. This must be combined with another MRI scan with different echo times in order to differentiate between the tissue types for a voxel-wise conversion [15]. Thus, UTE imaging could be a preferable method for some applications of MR-only RT, such as brain RT, since in theory it could provide intensity-based density value assignment without relying on prior knowledge or assumptions about the anatomy. In practice, for larger FOV, and most MR-only applications, the method becomes impractical due to long scan time and sensitivity to hardware imperfections and noise. Long scan time makes the method prone to segmentation errors due to intrascan motion [7].

MRI-based treatment planning – clinical implementation

Export to treatment planning systems

At the MRI scanner, all MR-RT image data is labeled as “MRI” in the DICOM modality tag. Upon export to a DICOM node, such as a PACS or a treatment planning system (TPS), the modality of the MRCAT image is changed to CT. During the export process, CT-specific DICOM attributes are added to the DICOM header and the resulting MRCAT image set appears as a CT image set (see Figure 11). Import of such data into the TPS is thereby analogous to importing CT data, with no manual post-processing required. The import has been tested to work with Pinnacle³ (version 9.10), Monaco (version 5), and Eclipse (version 11) planning systems.

Image fusion and organ delineation

One major benefit of MR-only simulation becomes evident at the start of treatment planning: the MRCAT and other MR scans share the same coordinate system, making additional registration unnecessary. Organ delineation algorithms in TPS typically use the CT information which is quantized in the MRCAT image. This allows for easy delineation of body outline and bones. The fatty outlines of the inner organs make some delineation algorithms able to build adequate first guesses of the location of bladder, prostate, and rectum, but T2W MR images are the necessary and best source for that purpose. The locations of seeds must be transferred to graphical elements and made available at the treatment machine at the time of image-based position adjustments.

DRR generation

For beam planning purposes, digitally reconstructed radiographs (DRRs) can be created from any direction in a way similar to CT, and the result is hard to distinguish visually from true CT DRRs (see Figure 12).

Dose planning

The workflow in dose planning for EBRT with MRCAT images does not differ from the use of plain CT images. The dosimetric accuracy for an MR-only simulation approach has been reported in multiple articles for several anatomies [7]. All studies report differences of less than 2% compared to CT-based calculation.

Together with the Netherlands Cancer Institute in Amsterdam, we performed our own study to compare MRCAT-based dosimetry with CT-based dosimetry. We used datasets from thirteen patients with an indication for prostate-only radiation treatment (10) and prostate plus lymph node radiation treatment (3). For those patients, the usual CT-based planning process was performed using the Philips Pinnacle³ treatment planning system, CT images from a Siemens Sensation Open

scanner, and MR images from a Philips Achieva TX 3T system. In addition to the clinical MR protocol, the patients received an mDixon scan according to the protocol in Table 1. Using this mDixon scan, the MRCAT images were generated, registered onto the planning CT images, and the plan was recalculated. Since the differences in body contour due to variations in patient positioning would confound the results, the following



Figure 11: Upon export to TPS, the MRCAT image becomes a CT-type image with HU values for water, air, compact bone, spongy bone, and adipose tissue.



Figure 12: Comparison of DRRs based on MRCAT-based pseudo CT (left) and planning-CT (right)

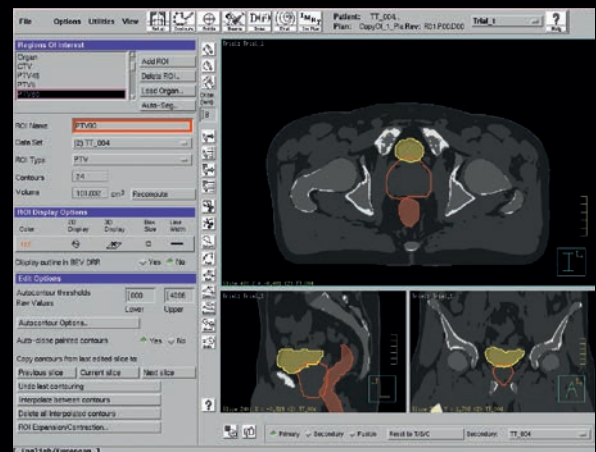


Figure 13A: MRCAT imaging data imported in Pinnacle³ with delineations for treatment planning

procedure to match the body contour between the CT and MR images was applied: First, the body contour was segmented in the CT images using a combination of threshold-based segmentation using -200HU as threshold and morphological operations. Then the segmentation was taken over to the MRCAT images. Regions in the MRCAT image outside of the body contour were set to air values. Regions in the MRCAT image within the body contour which had air values assigned were re-assigned water values, i.e. “empty” areas in the MRCAT within the CT outline were “filled with water.” All patients were planned for VMAT treatments using two arcs of 280° each.

The dose calculation differences were evaluated using a gamma analysis [16] with both a 3%/3 mm and a 1%/1 mm criterion. Figure 13 shows a sample case. Considering the volume receiving 75% of the maximum dose or more, on average 99.99% of the voxels had a gamma value smaller than 1, in other words - they would pass the gamma criterion. The median 3%/3 mm gamma value over this volume ranged in this patient population from 0.05 to 0.15 with an average of 0.08; the 99% quantile of the gamma values within this volume ranged from 0.16 to 0.33 with an average of 0.22. For the 1%/1 mm analysis the values were 99.83% of voxels with gamma smaller than 1 (range 99.01% to

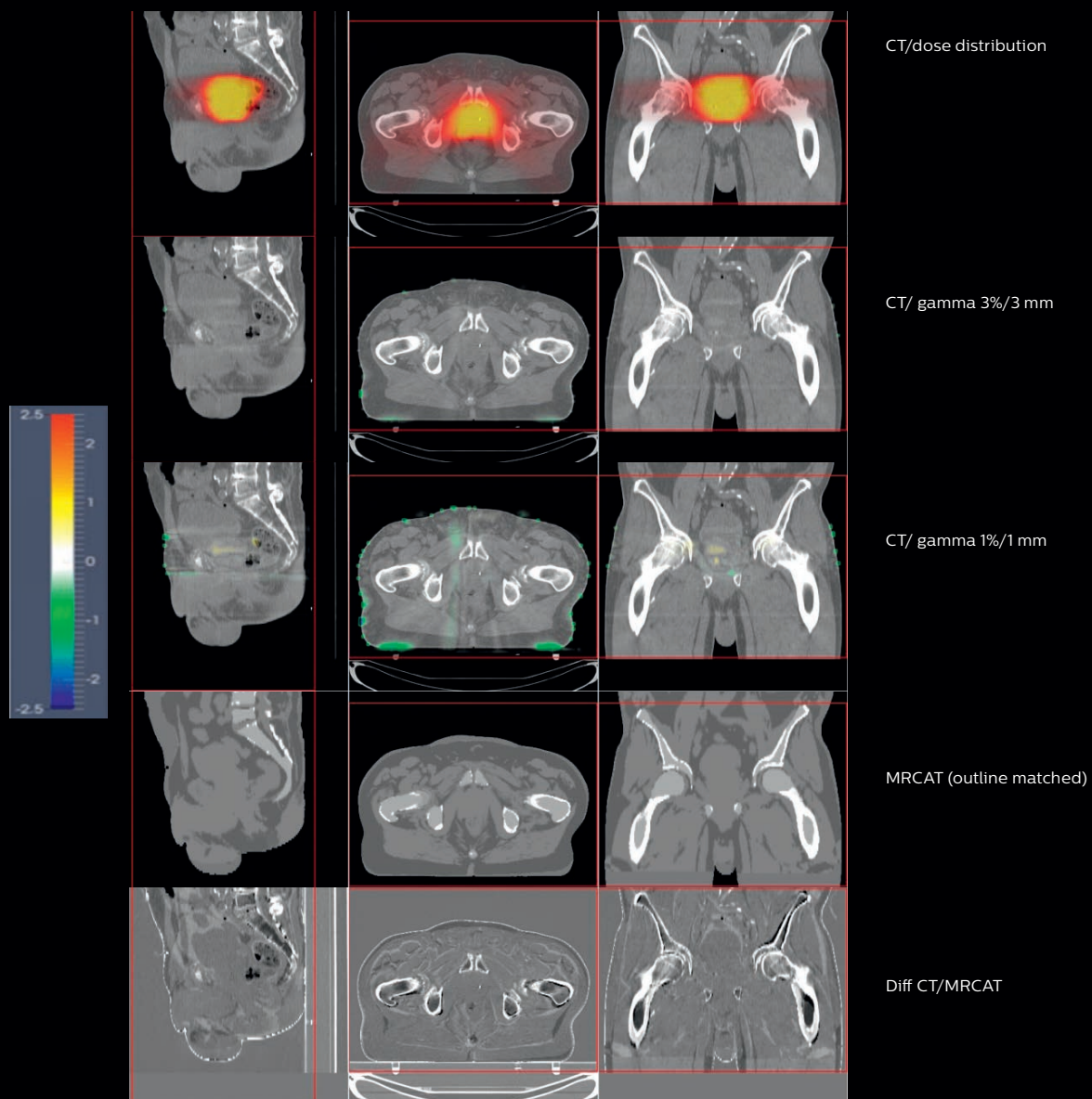


Figure 13B: Example of the visualization of dose differences. Left, center, and right column show sagittal, axial, and coronal views respectively. The first row shows the dose distribution as overlay over the original CT image, the second and third row show the 3%/3 mm and 1%/1 mm gamma distributions overlaid over the CT image (where red and blue in the overlay represent +1 and -1 respectively), the fourth row shows the MRCAT image, and the fifth row shows a difference image between the MRCAT and the CT image in order to demonstrate the registration accuracy. The color scale is for the gamma overlays; note that the opacity drops from 50% at +/-1 to 0% at 0.

100%), median gamma 0.20 (range 0.11 to 0.43), 99% quantile of gamma 0.65 (range 0.46 to 0.99). This indicates that dosimetry using MRCAT images yields results well within clinical tolerance limits. In addition, dose-volume histograms (DVH) were evaluated. For the organs at risk, the mean dose was computed on the MRCAT images on average 0.42% lower compared to the original CT (standard deviation 0.50%); for the target structures the difference was on average 0.25% lower (standard deviation 0.17%). This is also well within clinical tolerance limits.

Clinical example

A 76-year-old prostate cancer patient (Gleason score 7 (3+4), PSA 17,2 µg/l) receiving EBRT at the Docrates Cancer Center in Helsinki, Finland was scanned for evaluation of the MR-only workflow with Philips MRCAT. The study protocol was approved by the Helsinki University Hospital Coordinating Ethics Committee. For comparison to the clinical RT plan, the plan was recalculated on MRCAT images with identical monitor units (MU). Identical planning target volume and OAR delineations were used for both plans (see Figure 14) on Pinnacle³ and Eclipse TPS systems. Dose calculation accuracy was assessed based on dose volume histograms (DVHs). Agreement was good in both TP systems. In Pinnacle³, for the Planned Target Volume (PTV), 3D mean dose was increased from 7809.9 cGy to 7810.7 cGy and maximum decreased from 8117.6 cGy to 8089.3 cGy,

with CT and MRCAT, respectively. For the target DVH curve points D99% and D1% the difference was negligible. Minor differences can be seen between OAR DVHs (see Figure 15).

MR images used as a source for MRCAT calculation were taken during a separate imaging session. Thus, patient position and body outline are not completely identical in the two image sets compared here. Slight changes will also occur between treatment fractions. These differences are likely to explain, together with interscan organ motion, the differences seen in the dose distribution (see Figure 15).

MR-only based planning

MR-only based plans were then made by an experienced radiation oncologist to illustrate the impact of MR-based delineation to the plan quality (see Figure 16). It has been reported in several studies (such as the one described by C. C. Parker [17]) that if the PTV would be drawn using the same rules as for CT the size of the PTV would shrink, because the PTV conforms more closely to the actual prostate outline. However, the actual clinical value of reduced target volume should be shown by long-term clinical follow-up. In this particular example, the original PTV was also affected by a choline PET/CT study that was obtained for improved target characterization.

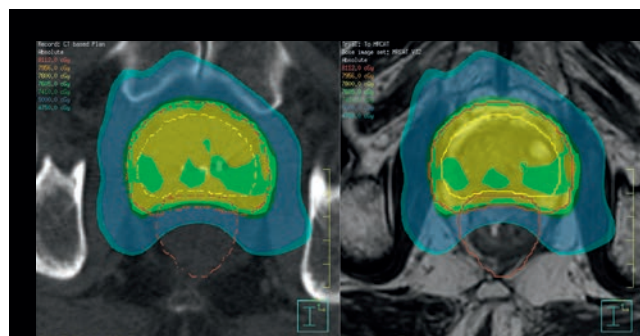


Figure 14: Comparison of dose distribution on MRCAT (right) and planning CT (left)

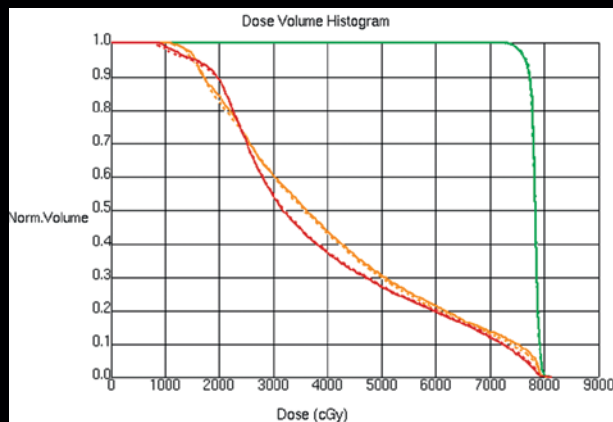


Figure 15: Dose volume histogram for PTV (green), bladder (yellow), and rectum (red). The dashed lines indicate the CT-based plan and solid the MRCAT-based plan.

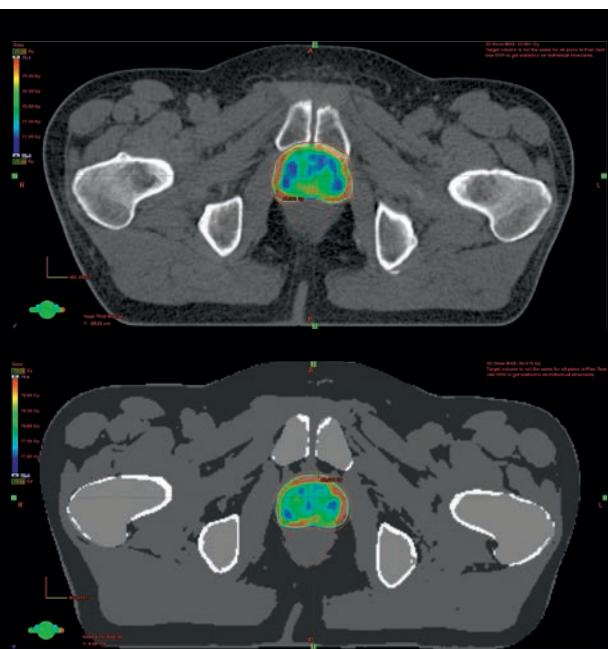


Figure 16: A comparison of original CT-based (top) and MR-only based plans (bottom) illustrates the impact of MR-based delineation to the size of the prostate and consequently the PTV. (Image courtesy of Docrates Cancer Center, Helsinki, Finland).

Workflow considerations

Overall, MR-only simulation uses a workflow similar to CT simulation. This chapter describes some specific aspects to consider when commissioning MR-only simulation.

Imaging in the treatment position

MR-only simulation is contingent on the patient imaged in the RT treatment position. For this, the flat, indexed Ingenia MR-RT CouchTop accommodates many common positioning device solutions. With knee positioning devices, the position of femurs and pelvic bones can be set the same way as in the treatment machine. Indexing bars allow other equipment to be attached to the indexed locations on the MR CouchTop.

For high SNR, the Anterior and Posterior coil should be positioned as close to the anatomy as possible, but without deforming body contours. The MR-RT CouchTop is 2.5 cm thinner than the previous overlay solution, thereby bringing the patient as close as possible to the underlying Posterior coil. Another advantage of the CouchTop versus the overlay solution is that this one-piece approach eliminates mechanical play of up to few millimeters between the overlay and the table system.



Figure 17: Top: Prostate patient positioned on MR-RT CouchTop. Bottom: Coil Support can be easily adjusted and tilted

The Anterior Coil Support can be easily adjusted and tilted. The spacious design of the coil support makes optimal use of the bore space and enables imaging of also large patients (see Figure 17).

Patient marking

MR-only simulation supports relative marking with the external laser positioning system (ELPS). Marks can be made to the approximate reference location before the patient is transferred to the isocenter (see Figure 18). The open design of the Coil Support and the option to slide it freely allows laser projections from virtually any direction onto the target area. With the one-click travel-to-scan feature, additional alignment with the MR façade laser is unnecessary

Use of MR-visible location markers on top of the relative skin marks during scanning is advised. The temporary marks can later be replaced with permanent tattoos, for example before the first fraction. Tattooing near the MRI scanner bore is not advisable.

Position verification

The patient can be aligned at the treatment machine using the skin marks, but the position should be fine-tuned and verified with one of three image-based options: cone-beam computed tomography (CBCT), plain radiographs against the bone information indicated in the DRRs, or the graphically or numerically recorded location of internal prostate markers.



Figure 18: Patient marking at the MR scanner using the ELPS

Conclusions and future outlook

MR simulation for RT treatment planning has gained interest in the quest for more accurate target definition, based on its excellent soft-tissue contrast and accurate 3D imaging capabilities. In addition, as explained in this paper, MR-only simulation for the prostate is introduced as an aid to the treatment planning process without the explicit need for CT simulation. By just adding a few minutes to the MR simulation exam, the density information that was needed from CT for dose planning can be obtained through MRI. MR-only simulation fits well in a radiation oncology department's workflow and is the cornerstone for next applications which aim to benefit from the advantages of MRI. We believe MR-only simulation is an important step toward the adoption of MRI in radiation treatment planning. In anticipation of therapy treatments based on MRI, such as MR-Linac² and adaptive treatments, we even believe that MR-only simulation is indispensable for accurate matching of MRI to MRI data.

Acknowledgements

Uulke van der Heide, PhD and Marloes Frantzen, from the Netherlands Cancer Institute, Amsterdam, the Netherlands for their validation work of the MRCAT algorithms and provision of the data

Timo Kiljunen, PhD, from the Docrates Cancer Center, Helsinki, Finland for setting up, and executing the clinical trial on MRCAT generation

Abbreviations and terminology

CT	Computed Tomography
CBCT	Cone-beam Computed Tomography
DRR	Digitally Reconstructed Radiograph
DVH	Dose Volume Histogram
EBRT	External Beam Radiation Therapy
ELPS	External Laser Positioning System
FOV	Field of View
HU	Hounsfield Unit
IMRT	Intensity Modulated Radiation Therapy
MRCAT	Magnetic Resonance for Calculating Attenuation
MR-only simulation	The use of MR images to support radiation therapy planning as a primary image set
MRI	Magnetic Resonance Imaging
MU	Motor Units
OAR	Organs at Risk
PTV	Planned Target Volume
RT	Radiotherapy or Radiation Therapy
SNR	Signal-to-Noise Ratio
TPS	Treatment Planning System
VMAT	Volumetric Modulated Arc Therapy

² MR-Linac is a collaboration between Elekta and Philips [18] and is currently works-in-progress.

Bibliography

- [1] P. Dirix, K. Haustermans, and V. Vandecaveye, "The Value of Magnetic Resonance Imaging for Radiotherapy Planning," *Semin. Radiat. Oncol.*, vol. 24, no. 3, pp. 151–159, Jul. 2014.
- [2] G. P. Liney and M. A. Moerland, "Magnetic Resonance Imaging Acquisition Techniques for Radiotherapy Planning," *Semin. Radiat. Oncol.*, vol. 24, no. 3, pp. 160–168, Jul. 2014.
- [3] E. S. Paulson, B. Erickson, C. Schultz, and X. Allen Li, "Comprehensive MRI simulation methodology using a dedicated MRI scanner in radiation oncology for external beam radiation treatment planning," *Med. Phys.*, vol. 42, no. 1, pp. 28–39, Jan. 2015.
- [4] J. Ferlay, E. Steliarova-Foucher, J. Lortet-Tieulent, S. Rosso, J. W. W. Coebergh, H. Comber, D. Forman, and F. Bray, "Cancer incidence and mortality patterns in Europe: Estimates for 40 countries in 2012," *Eur. J. Cancer*, vol. 49, no. 6, pp. 1374–1403, Apr. 2013.
- [5] C. Tsien, Y. Cao, and T. Chenevert, "Clinical applications for diffusion magnetic resonance imaging in radiotherapy," *Semin. Radiat. Oncol.*, vol. 24, no. 3, pp. 218–226, Jul. 2014.
- [6] "Determination of Absorbed Dose in a Patient Irradiated by Beams of X or Gamma Rays in Radiotherapy Procedures. ICRU Report 24." ICRU, 1976.
- [7] T. Nyholm and J. Jonsson, "Counterpoint: Opportunities and Challenges of a Magnetic Resonance Imaging–Only Radiotherapy Work Flow," *Semin. Radiat. Oncol.*, vol. 24, no. 3, pp. 175–180, Jul. 2014.
- [8] C. Bos, M. A. Viergever, and C. J. G. Bakker, "On the artifact of a subvoxel susceptibility deviation in spoiled gradient-echo imaging," *Magn. Reson. Med.*, vol. 50, no. 2, pp. 400–404, Aug. 2003.
- [9] "ICRU 23. Measurement of Absorbed Dose in a Phantom Irradiated by Single Beams of X or Gamma Rays (1973)."
- [10] "ICRU 44. Tissue Substitutes in Radiation Dosimetry and Measurement (1989)."
- [11] "ICRU 46. Photon, Electron, Proton and Neutron Interaction Data for Body Tissues (1992)."
- [12] O. Ecabert, J. Peters, H. Schramm, C. Lorenz, J. von Berg, M. J. Walker, M. Vembar, M. E. Olszewski, K. Subramanyan, G. Lavi, and J. Weese, "Automatic Model-Based Segmentation of the Heart in CT Images," *Ieee Trans. Med. Imaging*, vol. 27, no. 9, pp. 1189–1201, Sep. 2008.
- [13] J. A. Dowling, J. Lambert, J. Parker, O. Salvado, J. Fripp, A. Capp, C. Wratten, J. W. Denham, and P. B. Greer, "An Atlas-Based Electron Density Mapping Method for Magnetic Resonance Imaging (MRI)–Alone Treatment Planning and Adaptive MRI–Based Prostate Radiation Therapy," *Int. J. Radiat. Oncol.*, vol. 83, no. 1, pp. e5–e11, May 2012.
- [14] M. Hofmann, F. Steinke, V. Scheel, G. Charpiat, J. Farquhar, P. Aschoff, M. Brady, B. Scholkopf, and B. J. Pichler, "MRI-Based Attenuation Correction for PET/MRI: A Novel Approach Combining Pattern Recognition and Atlas Registration," *J. Nucl. Med.*, vol. 49, no. 11, pp. 1875–1883, Oct. 2008.
- [15] A. Johansson, "CT substitute derived from MRI sequences with ultrashort echo time." *Med. Phys.*, vol. 3, no. 5, pp. 2708–2714, 2011.
- [16] D. A. Low, W. B. Harms, and S. Mutic, "A technique for the quantitative evaluation of dose distributions," *Med. Phys.*, vol. 25, no. 5, pp. 656–61, 1998.
- [17] C. C. Parker, A. Damyanovich, T. Haycocks, M. Haider, A. Bayley, and C. N. Catton, "Magnetic resonance imaging in the radiation treatment planning of localized prostate cancer using intra-prostatic fiducial markers for computed tomography co-registration," *Radiother. Oncol. J. Eur. Soc. Ther. Radiol. Oncol.*, vol. 66, no. 2, pp. 217–224, Feb. 2003.
- [18] "Press Release. Dutch medical center begins installation of world's first high-field MRI-guided radiation therapy system. April 6, 2014".

© 2015 Koninklijke Philips N.V. All rights reserved.
Specifications are subject to change without notice.
Trademarks are the property of Koninklijke Philips N.V.
(Royal Philips) or their respective owners.

4522 991 11581 * JUN 2015



Ingenia MR-RT is not available in all countries. MR-only simulation is not available in all countries and for all configurations. Please contact your local Philips representative for further details.

This material is not intended for distribution in the U.S.A.

How to reach us:
Please visit www.philips.com/mr-rt
healthcare@philips.com